



Formation of Halogen-bearing Species. II. Irradiation of Chloromethane in Carbon Monoxide Ice with VUV Light and Electrons

Meng-Yeh Lin¹, Tzu-Ping Huang¹, Pei-Zhen Wu¹, Chih-Hao Chin¹, and Yu-Jong Wu^{1,2}

¹ National Synchrotron Radiation Research Center, No. 101, Hsin-Ann Road, Hsinchu Science Park, Hsinchu 30076, Taiwan; yjwu@nsrrc.org.tw

² Department of Applied Chemistry and Institute of Molecular Science, National Chiao Tung University, 1001, Ta-Hsueh Road, Hsinchu 30010, Taiwan

Received 2019 August 7; revised 2019 November 14; accepted 2019 November 16; published 2020 January 6

Abstract

The synthesis of chlorine-bearing species in CO ice was studied by the irradiation of CH₃Cl:CO ice at 10 K with vacuum-ultraviolet (VUV) light and energetic electrons. In contrast to the photochemical behavior of CH₃F:CO ice, photolysis of CH₃Cl:CO ice with Ly α or broadband VUV light afforded various products. This discrepancy was attributed to the abundant absorption bands of CH₃Cl in the VUV region, particularly in the Ly α region. The Cl-bearing species including Cl₂O, ClCO, C₃Cl₂, C₃HCl, and HOCl were characterized by observing their IR features. In contrast, electron bombardment of ice mixtures produced various carbon oxides and primary products, such as CH₂Cl and HCO. In addition, the mechanism of energetic processes in electron bombardment was discussed.

Unified Astronomy Thesaurus concepts: Astrochemistry (75); Molecular spectroscopy (2095); Line positions (2085); Molecule formation (2076); Galaxy chemical evolution (580); Chemical abundances (224)

1. Introduction

The detection of CH₃Cl around small-mass protostar IRAS 16293-2422 observed by the Atacama Large Millimeter/submillimeter Array and in the coma of comet 67P/Churyumov-Gerasimenko by the *Rosetta* mission was recently reported (Fayolle et al. 2017). This first detection of organohalides stimulates interest in the existence of other halogen-bearing species in space, as only simple halogen hydrides have been previously found in the interstellar environment. These species, including HF, CF⁺, HCl, HCl⁺, and H₂Cl⁺, have been found in diverse astrophysical environments (Blake et al. 1985; Schilke et al. 1995; Zmuidzinas et al. 1995; Neufeld et al. 1997, 2006, 2010, 2012, 2015; Cernicharo et al. 2010; Lis et al. 2010; Peng et al. 2010; Phillips et al. 2010; De Luca et al. 2012; Muller et al. 2014; Kawaguchi et al. 2016); however, compared to H-, C-, O-, and N-containing species in space, halogen-containing species have attracted less attention in the astrochemical community.

Laboratory simulations of interstellar ice containing the newly found organohalides by photolysis and radiolysis are essential so that they might produce other halogen-bearing species, which could be potential targets for future astronomical surveys. In addition, the formation of molecules might be distinguished by various energetic processes that provide useful information for the understanding of the local astrophysical environmental conditions via the detection of specific species. In our previous study (Lin et al. 2019), a CO ice sample containing CH₃F in small proportion was prepared at 10 K, and its chemistry was compared by irradiation with vacuum-ultraviolet (VUV) photons and energetic electrons. CO represents one of the most abundant species of ice grains in the interstellar medium (ISM), and CO freeze-out occurs deeper in dense clouds ($A_V \geq 3$), forming apolar ice (Boogert et al. 2015). The results revealed that the electron irradiation of the CH₃F:CO ice sample produces products more different than those produced by VUV photolysis due to the sufficient energy provided by electron bombardment to dissociate or ionize CO and CH₃F species, thereby opening various reaction channels.

In contrast, CO is nearly transparent to Ly α light, and its dissociation or ionization requires energy greater than 11.1 eV (~ 112 nm). Although CH₃F exhibits continuous absorption at wavelengths of less than 150 nm, absorption cross sections are generally less than 2×10^{-17} cm² (Locht et al. 2000). These factors limit the formation of complex fluorine-bearing molecules upon VUV photolysis of CH₃F:CO ice at a total photon dose of 10^{17} photons. In this study, our study was extended to CH₃Cl:CO ice exposed to VUV light and 3 keV electrons and compared with the results obtained in our previous study on CH₃F:CO (Lin et al. 2019).

2. Experimental Methods

The experimental setup was described elsewhere (Wu et al. 2012; Chin et al. 2016; Lin et al. 2019). A copper plate was coated with polished nickel, which served as a substrate, for the deposition of ice samples, and a mirror for reflection of the incident IR beam to a detector. The cryochamber was evacuated to a pressure of less than 1×10^{-8} torr in advance, followed by cooling the substrate using a closed-cycle helium refrigerator system (ARS DE-204) for the deposition of an ice sample.

A gaseous CH₃Cl:CO (1:250) sample was prepared and directly introduced into the cryochamber for deposition at 10 K over 2 hr at a flow rate of 1.0 mmol hr⁻¹. The ice sample thickness was estimated to be 10 μ m by the IR interference fringe measurement (Zondlo et al. 1997; Jamieson et al. 2006). The substrate temperature was measured with an accuracy of ± 0.1 K using a temperature controller (Lakeshore 331S) with a calibrated silicon diode (DT-470).

The electron beam (energy = 3 keV and flux = 1.5×10^{14} electrons s⁻¹) was generated using an electron gun (Kimball Physics, Model EFG-7) for radiolysis of the ice sample. The penetration depth of incident electrons was expected to be less than 0.5 μ m (Bennett et al. 2013), such that only the upper layers of the ice sample would interact with incident electrons. In addition, two light sources were used for photolysis experiments: Ly α light (flux $\approx 5 \times 10^{12}$ photons

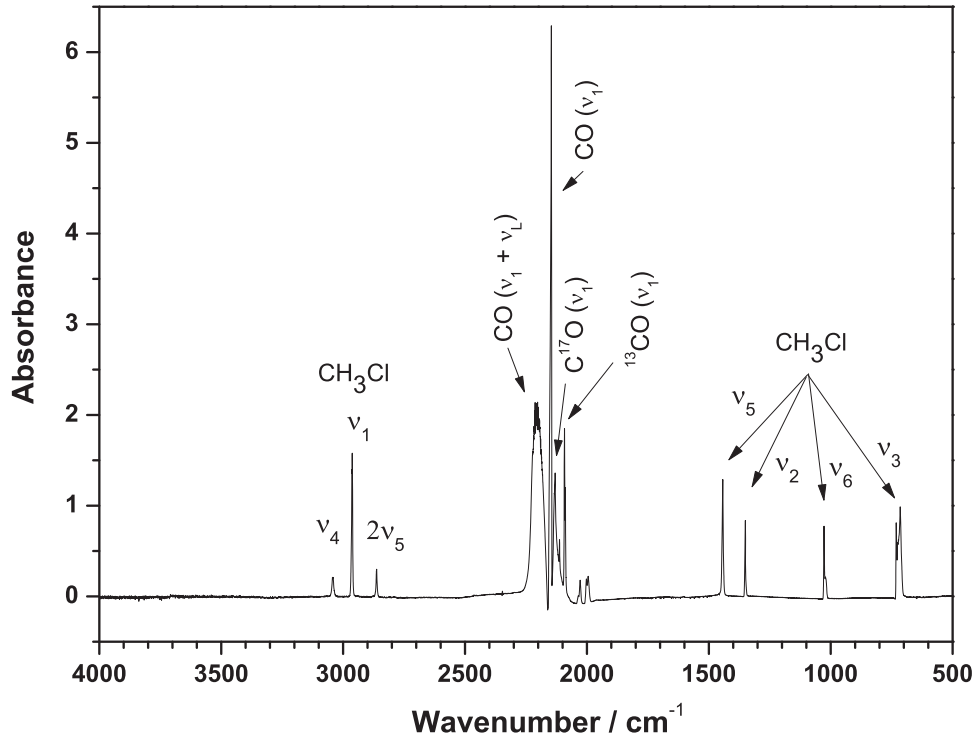


Figure 1. IR absorption spectrum of the CH₃Cl:CO (1:250) ice sample at 10 K.

s⁻¹, bandwidth ≈ 1.5 nm), generated from a synchrotron facility (Taiwan Light Source, TLS-03 beamline), and a broadband D₂ lamp (flux = $\sim 3 \times 10^{13}$ photons s⁻¹, Hamamatsu, Model L10366), providing a weak continuum emission in the 115–200 nm wavelength range, with characteristic emissions near 160 nm. In photolysis experiments, the total accumulated photon dose on ice samples was controlled to reach 10^{17} photons. Such a UV dose corresponds to more than 10^6 years in the ISM, which is equivalent to the timescale of a typical protostellar phase. Hence, irradiation times are ~ 5.5 hr, 55 minutes, and 11 minutes for the synchrotron light experiment, broadband light experiment, and 3 keV electron experiment, respectively. Then, the effects of irradiation of 121.6 nm photons, broadband photons, and 3 keV electrons were qualitatively compared.

Reflection IR absorption spectra of each stage in the experiments covering the 500–4000 cm⁻¹ spectral region at a resolution of 0.5 cm⁻¹ were measured by an FTIR spectrometer (Bruker, Vertex 80), equipped with a KBr beam splitter and MCT-B detector (cooled to 77 K). Gaseous CH₃Cl (99.5%, Matheson) and CO (99.9995%, Matheson) were used without further purification.

3. Results and Discussion

3.1. IR Absorption Spectra of CH₃Cl:CO Ice at Various Temperatures

Figure 1 shows the IR absorption spectrum of the CH₃Cl:CO ice mixture at 10 K. The IR absorption of pure CO ice has been studied extensively (Hudgins et al. 1993; Jamieson et al. 2006). Sharp and intense peaks at 2145, 2131, 2092, and 2088 cm⁻¹ corresponded to the ¹²C¹⁶O, ¹²C¹⁷O, ¹³C¹⁶O, and ¹²C¹⁸O stretching modes of CO, respectively. The broad band observed near 2208 cm⁻¹ with a bandwidth of ~ 45 cm⁻¹ corresponded to the ($\nu_1 + \nu_L$) mode of solid CO. Single sharp lines observed at

3042, 2963, 2863, 1442, and 1350 cm⁻¹ corresponded to the ν_4 (CH asymmetric stretching), ν_1 (CH symmetric stretching), $2\nu_5$, ν_5 (CH₃ asymmetric deformation), and ν_2 (CH₃ symmetric deformation) modes of CH₃Cl, respectively (Jacox & Milligan 1970; Binbrek & Anderson 1979). The intense absorption line observed at 1027 cm⁻¹ with a shoulder at 1021 cm⁻¹ corresponded to the ν_6 (CH₃ rocking) mode; the ratio of the observed intensities between the peak and shoulder was ~ 3 ; this ratio is similar to the natural isotopic ³⁵Cl/³⁷Cl abundance ratio. The C–Cl stretching mode (ν_3) was observed ~ 715 cm⁻¹ with a broad band. Similar behavior was observed in our previous study of the CH₃F:CO system (Lin et al. 2019), which was related to the interaction between nearby CO molecules and CH₃Cl along the C–Cl bond. The peak observed at 2028 cm⁻¹ corresponded to $2\nu_3$ of CH₃Cl. Doublet peaks observed at 2002 and 1995 cm⁻¹ corresponded to the absorptions of the CO-CH₃Cl complex, as the absorptions were absent in the cases of pure solid CO and the CH₃Cl/Ar matrix.

3.2. Photolysis with VUV Light

Jacox & Milligan (1970) have performed VUV photolysis of CH₃Cl in an Ar matrix with a hydrogen-discharge flow lamp, and CH₂Cl, CH₃, CH₂Cl₂, HCCl, CCl, HCCl₂, CH₄, and HCl were identified as the photolysis products. In the gaseous phase, the photolysis of CH₃Cl with VUV light leads to the main dissociation of the C–Cl bond and produces CH₃ radical and atomic Cl (Kawasaki et al. 1984; Matsumi et al. 1992; Brownsword et al. 1997; Lin et al. 2002). In contrast, CH₃ radicals were only found in a small proportion upon photolysis of CH₃Cl in a solid matrix. The Cl atom was observed to be present in most products, indicative of the difficulty in the detachment of the Cl atom upon VUV photolysis in a matrix environment (Jacox & Milligan 1970).

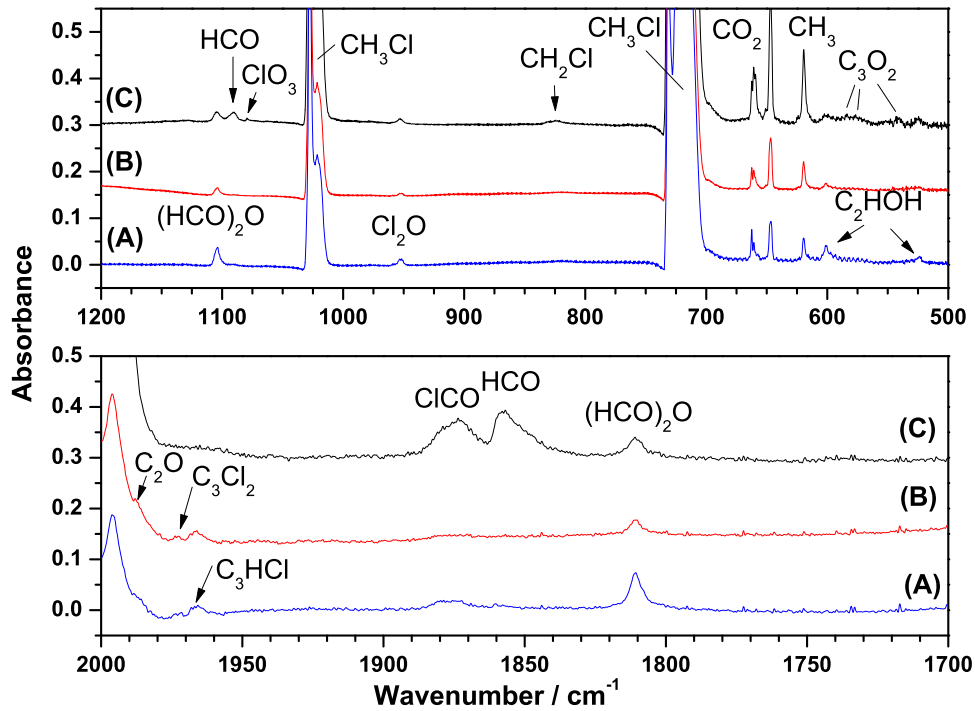


Figure 2. IR spectra recorded after irradiation of $\text{CH}_3\text{Cl}:\text{CO}$ ice samples at 10 K in separate experiments with (A) 121.6 nm, (B) broadband VUV light (D_2 lamp), and (C) 3 keV electrons. Traces (B) and (C) are offset for clarity.

In these photolysis experiments, we used light sources of two kinds: synchrotron radiation providing monochromatic light at 121.6 nm, and a D_2 lamp providing broad-band emission in the 115–200 nm range. Figures 2(A) and (B) show IR absorption spectra of $\text{CH}_3\text{Cl}:\text{CO}$ ice samples exposed to 121.6 nm and broadband VUV light, respectively. Similar products were observed in both cases, including C_2HOH , CH_3 , $(\text{HCO})_2\text{O}$ (formic anhydride), Cl_2O , ClCO , C_3Cl_2 , and C_3HCl , whereas C_2O , CH_2CHO (vinyl radical), and HOCl (chlorous acid) were formed only by broadband VUV photolysis (D_2 lamp). An absorption corresponding to HCl was expected to appear in the $2850\text{--}2870\text{ cm}^{-1}$ spectral region, but it was not observed; it might be too weak or it may overlap with the $2\nu_5$ band of CH_3Cl . Table 1 summarizes the observed lines and the corresponding assignments. Previous studies (Locht et al. 2001a, 2001b, 2001c; Eden et al. 2007) have reported that the photon energy at 121.6 nm exactly matches the absorption of CH_3Cl from the ground state to the $5p$ state; the photodissociation of gaseous CH_3Cl at 121.6 nm leads to the main formation of CH_3 , Cl , and H atoms (Brownsword et al. 1997; Amaral et al. 2001). The Cl atom can immediately react with the surrounding CO to form ClCO ; this reaction is exothermic by 28.9 kJ mol^{-1} (Nicovich et al. 1990). Hydrogenation of the surrounding CO is also expected to be efficient, as the hydrogenation of CO into H_2CO and CH_3OH is demonstrated experimentally (Watanabe & Kouchi 2002; Watanabe et al. 2004). Such reactions may also occur in our experiments; however, the formation efficiency of H_2CO and CH_3OH in this study may be considerably less than that in the experiments reported by Watanabe & Kouchi (2002) and Watanabe et al. (2004) because H atom bombardment was used in their experiments, while H atoms were the only photolysis products obtained herein, and hence much less abundant. H_2CO and CH_3OH were not identified among the products, but $(\text{HCO})_2\text{O}$ and C_2HOH were observed because not only hydrogen atoms

but also simple hydrocarbons were produced in CO ice upon photolysis of CH_3Cl in situ. The reactions of these fragments with surrounding CO were different from the proposed model for the successive hydrogenation of CO on ice surfaces. The observed weak lines corresponding to Cl_2O , C_3Cl_2 , and C_3HCl were generated by photolysis of $(\text{CH}_3\text{Cl})_2$ as diffusion of Cl atoms from their original sites of production was difficult.

Photolysis of the ice sample with broadband VUV light generated not only products similar to those produced by photolysis at 121.6 nm but also C_2O , CH_2CHO , and HOCl . The presence of C_2O generated upon VUV photolysis of CO ice and absence upon 121.6 nm photolysis has been discussed in detail elsewhere (Gerakines et al. 1996). Figure 3 shows the IR absorption spectra of the same samples as shown in Figures 2(A) and (B) in the $1200\text{--}1450\text{ cm}^{-1}$ spectral region. The lines observed at 1362 and 1380 cm^{-1} corresponded to HOCl and CH_2CHO , respectively. Yoshinobu et al. (2009) have studied the photolysis of $\text{HCl}:\text{O}_2$ in a Ne matrix. They reported the formation of O_3 , OCIO , ClOO , HOO , HOCl , and HOCl . They first identified the IR spectrum of HOCl , which is the most stable isomer of chlorous acid; the most intense line (HOO bending mode) of HOCl was observed as a multiple at $1359.6/1361.4/1361.9/1362.5/1363.6\text{ cm}^{-1}$, similar to our observation.

3.3. Radiolysis with Electrons

Kaiser et al. have extensively studied the electron bombardment of pure CO ice at 10 K with 5 keV electrons; the formation of various carbon chains (C_3 , C_6), carbon-chain monoxides (C_2O , C_3O , C_4O , C_5O , and C_6O or C_7O), CO_2 , and carbon suboxides (C_3O_2 , C_4O_2 , C_5O_2) was reported (Jamieson et al. 2006; Bennett et al. 2009a, 2009b, 2010; Förstel et al. 2016). In our previous study (Lin et al. 2019), the formation of CO_2 , C_2O , C_3O , C_3O_2 , and C_5O_2 upon 3 keV electron bombardment of $\text{CH}_3\text{F}:\text{CO}$ ice was characterized. In this study,

Table 1Wavenumbers/cm⁻¹ and Mode Assignments of New Lines Appearing after VUV Photolysis and Electron Bombardment of CH₃Cl:CO Ice Samples

| Ly α | Broad-band VUV | 3 keV Electron | Assignment | Reference ^a |
|-------------|--------------------------|--------------------------|---------------------------------------------------|------------------------|
| 524 | | 524 | C ₂ HOH | (1) |
| | | 542 | C ₃ O ₂ (ν_6) | (2) |
| | | 576 | C ₃ O ₂ ($\nu_6 + \nu_L$) | (2) |
| | | 582 | C ₃ O ₂ ($\nu_6 + \nu_L$) | (2) |
| 601 | 601 | 601 | C ₂ HOH | (1) |
| 619 | 619 | 619 | CH ₃ (ν_2) | (3) |
| 647 | 647 | 647 | CO ₂ -CH ₃ Cl | This work |
| | 662/661/659 ^b | 662/661/659 ^b | CO ₂ (ν_2) | (4) |
| | | 825 | CH ₂ Cl (ν_3) | (5) |
| 952 | 952 | 952 | Cl ₂ O (ν_1) | (6) |
| | | 1079 | ClO ₃ (ν_3) | (7) |
| | | 1090 | HCO (ν_2) | (8) |
| 1104 | 1104 | 1104 | (HCO) ₂ O (ν_7) | (9) |
| | 1362 | 1362 | HOOC (ν_2) ? ^c | (10) |
| | 1380 | 1380 | CH ₂ CHO (ν_6) | (11) |
| | 1526 | 1526 | CH ₂ CHO (ν_4) | (11) |
| | 1603 | 1603 | H ₂ O (ν_2) | (12) |
| 1811 | 1811 | 1811 | (HCO) ₂ O (ν_3) | (9) |
| | | 1858 | HCO (ν_3) | (8) |
| 1874 | 1874 | 1874 | ClCO (ν_1) | (13) |
| 1966 | 1966 | | C ₃ HCl (ν_2) | (14) |
| 1973 | 1973 | | C ₃ Cl ₂ (ν_1) | (14) |
| | 1987 | 1987 | C ₂ O (ν_1) | (2) |
| | 2062 | 2062 | C ₅ O ₂ (ν_5) | (15) |
| | 2242 | 2242 | C ₃ O ₂ (ν_3) | (2) |
| | 2248 | 2248 | C ₃ O (ν_1) | (2) |
| | 2348 | 2348 | CO ₂ (ν_3) | (15) |

Notes.

^a References: (1) Hochstrasser & Wirz (1989), (2) Jamieson et al. (2006), (3) Jacox (1977), (4) Ehrenfreund et al. (1997), (5) Jacox & Milligan (1970), (6) Chi & Andrews (1973) (7) Kopitzky et al. (2002), (8) Milligan & Jacox (1964), (9) Kuhne et al. (1979), (10) Yoshinobu et al. (2009), (11) Jacox (1982), (12) Hudson & Moore (1999), (13) Jacox & Milligan (1965), (14) Maier et al. (1994), (15) Förstel et al. (2016).

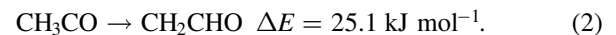
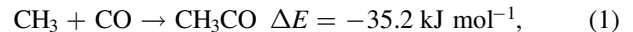
^b Triplet structure.

^c The question mark indicates the tentative assignment of the band.

CO₂, C₂O, C₃O, C₃O₂, and C₅O₂ were observed in similar proportions. This result is reasonable because similar concentrations of ice samples were used, and energetic electrons interacted mainly with the CO matrix.

Figure 2(C) shows the IR spectrum of the electron-bombarded ice sample in the region that clearly highlights differences of product formation between VUV photolysis and electron bombardment. Besides the abovementioned carbon oxides, radiolysis products were formed mainly from the primary fragments of CH₃Cl and the reactions of the primary fragments with the surrounding CO ice. Methyl radicals were found to be produced upon all energetic processing of the ice samples. An absorption line at 826 cm⁻¹ corresponding to chloromethyl radicals (CH₂Cl) was observed only in the electron-bombardment case. Their dissociation counterparts, Cl and H atoms, reacted with nearby CO to form ClCO and HCO, respectively. In addition, a weak line observed at 1079 cm⁻¹ corresponded to ClO₃ (Kopitzky et al. 2002). ClO₃ was absent upon VUV photolysis because the energy of the VUV photons was insufficient to break the CO bond to produce an individual O atom. Upon electron bombardment, CH₂CHO and HOOC (ν_2) molecules also were produced (Figure 3(C)). The former was

observed in the electron bombardment of CH₃F:CO ice, indicating a similar formation mechanism via the reaction of the primary hydrocarbon fragments with a CO molecule. The proposed mechanism is listed below (Miller et al. 2004; Tang et al. 2008) and will be discussed in the next section:



4. Comparison of Mechanisms between CH₃F and CH₃Cl in CO Ice Mixtures

The basic properties of these two ice systems are similar in the following ways: (1) CO ice is transparent to light of wavelength near 121.6 nm, (2) the dissociation threshold of CO is 11.1 eV, which is greater than the photon energy of the light source used for photolysis, and (3) 3 keV energetic electrons are used to the bombardment of mainly CO ice, the penetration depth of which is less than 0.5 μm . Hence, based on the abovementioned photophysical properties of CO, the photo-absorption of CH₃F and CH₃Cl in the VUV region plays an important role in photochemical reactions in CO ice. Previous studies (Locht et al. 2001a, 2001b, 2001c; Eden et al. 2007) have reported that the relative absorption cross sections of CH₃Cl are considerably greater than those of CH₃F over 115–165 nm. The C–Cl bond of CH₃Cl is also weaker than the C–F bond of CH₃F, indicating that higher energy is deposited into the fragments of CH₃ and Cl after photodissociation and that these activated fragments might possess sufficient energy to overcome the barrier for subsequent reactions with nearby CO molecules. Hence, a higher variety of products is obtained upon VUV photolysis of CH₃Cl in CO ice compared with that obtained for the CH₃F case in our previous study (Lin et al. 2019). An effective demonstration is CH₂CHO produced from the VUV photolysis of CH₃Cl:CO ice. Although the enthalpies of reactions (1) and (2) are not greater than those observed in the case of VUV photon energy, high-energy barriers for reactions (1) and (2) were reported to be 28.5 and 196 kJ mol⁻¹, respectively (Miller et al. 2004; Tang et al. 2008). The energy of a C–Cl bond is typically weaker than that of a C–F bond by 180 kJ mol⁻¹. Hence, the dissociation of the C–Cl bond of CH₃Cl with VUV light can allocate more remaining energy into the fragments than VUV photolysis of CH₃F.

Almost no difference in the formed products was observed with the photolysis of CH₃Cl:CO ice mixtures at 121.6 nm and broadband VUV light, except for HOOC (ν_2) and CH₂CHO molecules. The formation of these complex molecules observed only upon photolysis with broadband VUV light might indicate that simultaneous excitation of CH₃Cl and CO molecules is required to synthesize such complex molecules via multistep routes. The ionization energy of CH₃Cl is ~ 11.26 eV (~ 110.11 nm), but there is a reaction channel correlated to the production of the ion pair CH₃⁺ + Cl⁻ dissociated through the n_c3p_c Rydberg states with energy less than its ionization potential (de Medeiros et al. 2015). This effect might be another reason for the observation of the various photoproducts in the CH₃Cl:CO case.

Regarding the comparison to radiolysis experiments, the production of various carbon oxides did not exhibit any difference due to the main interaction of electron bombardment with dominant CO ice, but a clear difference in the formation of halogen-bearing species between the two cases was observed. When methyl halides were exposed to energetic electrons in

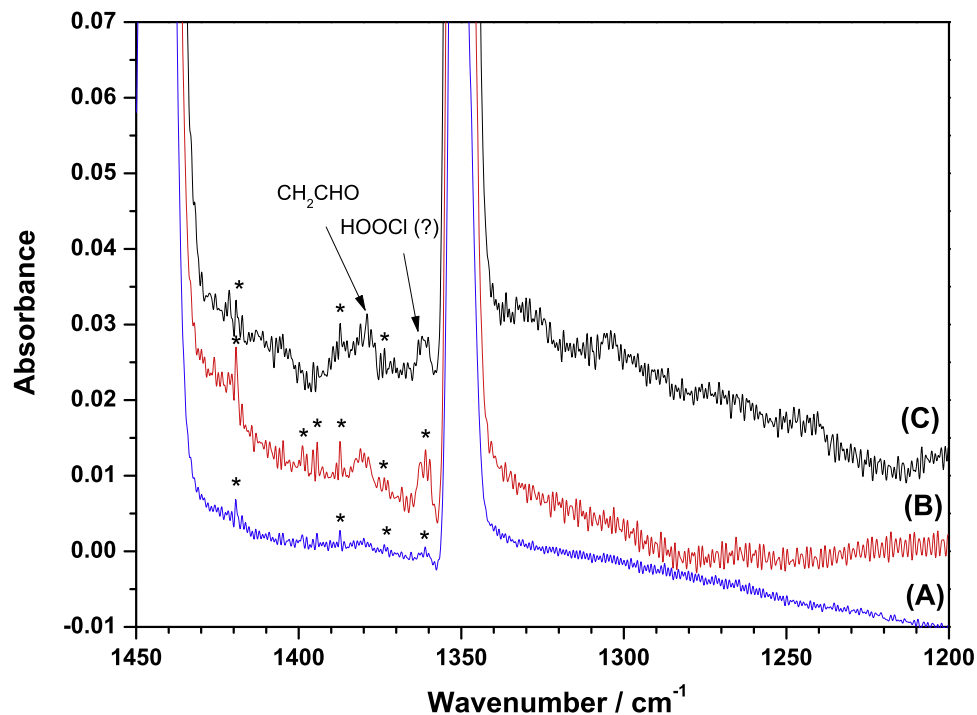


Figure 3. IR spectra recorded after irradiation of $\text{CH}_3\text{Cl}:\text{CO}$ ice samples at 10 K in separate experiments with (A) 121.6 nm, (B) broadband VUV light (D_2 lamp), and (C) 3 keV electrons. Traces (B) and (C) are offset for clarity. Lines marked * are attributed to atmospheric water absorptions. Although the IR optical paths are purged by dry N_2 during the experiments, the interference from the absorptions of atmospheric water cannot be clearly removed, leading to difficulty in peak assignments. Hence, the flow rate of dry N_2 is slightly adjusted at each stage to vary the amount of atmospheric water, which helps in distinguishing these peaks.

CO ice, the major dissociation channel was the dissociation of the carbon–halogen bond. F atoms are small, facilitating escape from the original CO cage to form CHF_3 and F_2CO . In contrast, Cl atoms, which are larger, would stay in the original site of production. The observed species containing more than one Cl atom were generated in the reactions of CH_3Cl clusters. Hence, these species are observed in a small proportion. Moreover, it is worth noting that the distribution of products might be different, if H_2O was also present in the ices. Since H_2O is the most abundant component of cold astrophysical ices and it has multiple roles in ice photochemistry (as a reactant, as a matrix, as a catalyst). Therefore, it is expected some of the products identified in the present work are formed in much lower abundances and/or react with surrounding H_2O molecules to form more complex species. Hence, they might be very difficult to detect with astronomical observations.

5. Conclusions

Energetic processes in $\text{CH}_3\text{Cl}:\text{CO}$ ice at 10 K were studied with VUV photolysis ($\text{Ly}\alpha$ line generated by a synchrotron beam and 115–200 nm range provided by a D_2 lamp) and 3 keV electron bombardment. The strong absorption of CH_3Cl in the VUV region led to its efficient dissociation and the production of various Cl-bearing photoproducts. This photochemical behavior was considerably different from the case of VUV photolysis of $\text{CH}_3\text{F}:\text{CO}$ ice. Besides the observation of the simple Cl-bearing species, such as ClCO , Cl_2O , C_3Cl_2 , and C_3HCl , the formation of HOOCI (chlorous acid) and H_2CCHO (vinyl oxy radical) was identified upon photolysis with the D_2 lamp, indicating that the synthesis of complex species might require the simultaneous excitation of both CH_3Cl and nearby CO molecules. Electron bombardment of similar ice also can generate HOOCI and other simple Cl-bearing species. In

addition, more primary products, including CH_2Cl , CH_3 , HCO , and ClCO , were preserved, probably due to some dissociation of CH_3Cl through a sequence of processes involving energy transfer and redistribution from energetic electrons to solid CO ice and then to CH_3Cl molecules. Hence, the remaining energy of the CH_3Cl fragments is marginal for further reactions to proceed.

Compared to the previous study on $\text{CH}_3\text{F}:\text{CO}$ ice, there was more opportunity to observe larger Cl-bearing species around the low-mass protostars or on comets because of the following reasons. (1) the absorption cross sections of CH_3Cl were greater in the VUV region, particularly near 121.6 nm. The dominant CO ice was (nearly) transparent to $\text{Ly}\alpha$ light and CH_3Cl was embedded, while the CH_3Cl species at any depth in the ice can be excited to highly excited states, from which further reactions proceeded with nearby species. (2) The energy of a C–Cl bond was typically less than that of a C–F bond by 180 kJ mol^{-1} , indicating that even though energetic particles do not directly bombard CH_3Cl , the effects, including secondary electrons and UV/VUV photon emissions from the ice, can still activate the C–Cl bond for further reactions.

The Ministry of Science and Technology of the Republic of China (grants MOST 106-2113-M-213-002-MY3 and 108-2639-M-009-001-ASP) and NSRRC provided financial support.

References

- Amaral, G., Xu, K., & Zhang, J. J. 2001, *JPCA*, **105**, 1115
- Bennett, C. J., Jamieson, C. S., & Kaiser, R. I. 2009a, *ApJS*, **182**, 1
- Bennett, C. J., Jamieson, C. S., & Kaiser, R. I. 2009b, *PCCP*, **11**, 4210
- Bennett, C. J., Jamieson, C. S., & Kaiser, R. I. 2010, *PCCP*, **12**, 4032
- Bennett, C. J., Pirim, C., & Orlando, T. M. 2013, *ChRv*, **113**, 9086
- Binbrek, O. S., & Anderson, A. 1979, *CPL*, **65**, 287

- Blake, G. A., Keene, J., & Phillips, T. G. 1985, [ApJ](#), **295**, 501
- Boogert, A. C. A., Gerakines, P. A., & Whittet, D. C. B. 2015, [ARA&A](#), **53**, 541
- Brownsword, R. A., Hillenkamp, M., Laurent, T., et al. 1997, [JChPh](#), **106**, 1359
- Cernicharo, J., Goicoechea, J. R., Daniel, F., et al. 2010, [A&A](#), **518**, L115
- Chi, F. K., & Andrews, L. 1973, [JPhCh](#), **77**, 3062
- Chin, C.-H., Chen, S.-C., Liu, M.-C., Huang, T.-P., & Wu, Y.-J. 2016, [ApJS](#), **224**, 17
- De Luca, M., Gerin, M., Falgarone, E., et al. 2012, [ApJ](#), **751**, 37
- de Medeiros, V. C., de Andrade, R. B., Leitão, E. F. V., et al. 2015, [JChS](#), **138**, 272
- Eden, S., Limão-Vieira, P., Hoffmann, S. V., & Mason, N. J. 2007, [CP](#), **331**, 232
- Ehrenfreund, P., Boogert, A. C. A., Gerakines, P. A., Tielens, A. G. G. M., & van Dishoeck, E. F. 1997, [A&A](#), **328**, 649
- Fayolle, E. C., Öberg, K. I., Jørgensen, J. K., et al. 2017, [NatAs](#), **1**, 703
- Förstel, M., Maksyutenko, P., Mebel, A. M., & Kaiser, R. I. 2016, [ApJL](#), **818**, L30
- Gerakines, P. A., Schutte, W. A., & Ehrenfreund, P. 1996, [A&A](#), **312**, 289
- Hochstrasser, R., & Wirz, J. 1989, [Angew. Chem.](#), **101**, 183
- Hudgins, D. M., Sandford, S. A., Allamandola, L. J., & Tielens, A. G. G. M. 1993, [ApJS](#), **86**, 173
- Hudson, R. L., & Moore, M. H. 1999, [Icar](#), **140**, 451
- Jacox, M. E. 1977, [JMoSp](#), **66**, 272
- Jacox, M. E. 1982, [CP](#), **69**, 407
- Jacox, M. E., & Milligan, D. E. 1965, [JChPh](#), **43**, 866
- Jacox, M. E., & Milligan, D. E. 1970, [JChPh](#), **53**, 2688
- Jamieson, C. S., Mebel, A. M., & Kaiser, R. I. 2006, [ApJS](#), **163**, 184
- Kawaguchi, K., Muller, S., Black, J. H., et al. 2016, [ApJ](#), **822**, 115
- Kawasaki, M., Kasatani, K., Sato, H., Shinohara, H., & Nishi, N. 1984, [CP](#), **88**, 135
- Kopitzky, R., Grothe, H., & Willner, H. 2002, [CEJ](#), **8**, 5601
- Kuhne, H., Ha, T.-K., Meyer, R., & Gunthard, H. H. 1979, [JMoSp](#), **77**, 251
- Lin, J. J., Chen, Y., Lee, Y. Y., Lee, Y. T., & Yang, X. 2002, [CPL](#), **361**, 374
- Lin, M.-Y., Huang, T.-P., Wu, P.-Z., Chin, C.-H., & Wu, Y.-J. 2019, [ApJ](#), **880**, 132
- Lis, D. C., Phillips, T. G., Goldsmith, P. F., et al. 2010, [A&A](#), **521**, L9
- Locht, R., Leyh, B., Hoxha, A., et al. 2000, [CP](#), **257**, 283
- Locht, R., Leyh, B., Hoxha, A., et al. 2001a, [CP](#), **272**, 277
- Locht, R., Leyh, B., Hoxha, A., et al. 2001b, [CP](#), **272**, 293
- Locht, R., Leyh, B., Hoxha, A., Johsims, H. W., & Baumgärtel, H. 2001c, [CP](#), **272**, 259
- Maier, G., Preiss, T., Reisenauer, H. P., Hess, B. A., Jr., & Schaad, L. J. 1994, [JChS](#), **116**, 2014
- Matsumi, Y., Das, P. K., & Kawasaki, M. 1992, [JChPh](#), **97**, 5261
- Miller, J. L., McCunn, L. R., Krisch, M. J., Bulter, L. J., & Shu, J. 2004, [JChPh](#), **121**, 1830
- Milligan, D. E., & Jacox, M. E. 1964, [JChPh](#), **41**, 3032
- Muller, S., Black, J. H., Guélin, M., et al. 2014, [A&A](#), **566**, L6
- Neufeld, D. A., Black, J. H., Gerin, M., et al. 2015, [ApJ](#), **807**, 54
- Neufeld, D. A., Roueff, E., & Snell, R. L. 2012, [ApJ](#), **748**, 37
- Neufeld, D. A., Schilke, P., Menten, K. M., et al. 2006, [A&A](#), **454**, L37
- Neufeld, D. A., Sonnentrucker, P., Phillips, T. G., et al. 2010, [A&A](#), **518**, L108
- Neufeld, D. A., Zmuidzinas, J., Schilke, P., & Phillips, T. G. 1997, [ApJL](#), **488**, L141
- Nicovich, J. M., Kreutter, K. D., & Wine, P. H. 1990, [JChPh](#), **92**, 3539
- Peng, R., Yoshida, H., Chamberlin, R. A., et al. 2010, [ApJ](#), **723**, 218
- Phillips, T. G., Bergin, E. A., Lis, D. C., et al. 2010, [A&A](#), **518**, L109
- Schilke, P., Phillips, T. G., & Wang, N. 1995, [ApJ](#), **441**, 334
- Tang, S., Ratliff, B. J., FitzPatrick, B. L., & Bulter, L. J. 2008, [JPCB](#), **112**, 16050
- Watanabe, N., & Kouchi, A. 2002, [ApJL](#), **571**, L173
- Watanabe, N., Nagaoka, A., Shiraki, T., & Kouchi, A. 2004, [ApJ](#), **616**, 638
- Wu, Y.-J., Wu, C. Y. R., Chou, S.-L., et al. 2012, [ApJ](#), **746**, 175
- Yoshinobu, T., Akai, N., Kawai, A., & Shibuya, K. 2009, [CPL](#), **477**, 70
- Zmuidzinas, J., Blake, G. A., Carlstrom, J., Keene, J., & Miller, D. 1995, [ApJL](#), **447**, L125
- Zondlo, M. A., Onasch, T. B., Washawsky, M. S., et al. 1997, [JPCB](#), **101**, 10887